

Constituent quark-light vector mesons effective couplings in a weak background magnetic field

Fábio L. Braghin

Instituto de Física, Federal University of Goiás, Av. Esperança, s/n, 74690-900 Goiânia, GO, Brazil

 (Received 26 September 2017; published 30 January 2018)

Effective couplings between light SU(2) vector and axial mesons and constituent quarks are calculated in the presence of a background electromagnetic field by considering a one dressed gluon exchange quark-quark interaction. The effective coupling constants, obtained from a large quark mass expansion, are expressed in terms of the Lagrangian parameters of the initial model and of components of the quark and nonperturbative gluon propagators. In spite of many possible couplings, only a few coupling constants emerge. As a second step, constituent quark-vector and axial mesons effective coupling constants are redefined to show explicit dependence on a weak background magnetic field. Ratios between the effective coupling constants are found in the limit of large quark effective mass and numerical estimates are presented.

DOI: [10.1103/PhysRevD.97.014022](https://doi.org/10.1103/PhysRevD.97.014022)

I. INTRODUCTION

Light vector mesons dynamics play an important role in intermediary energies nuclear and hadron phenomena. Although it could be expected that the mechanism for confinement could provide an unambiguous route for this program, it is not known. In this context the formulation of effective models has been one of the most important routes for the understanding of hadron and nuclear strong interactions by considering the related relevant symmetries. Chiral symmetry and its dynamical symmetry breaking (DChSB) are some of the essential ideas from phenomenology and QCD that have made possible great advances in the field. For example, approximated chiral symmetry favors the interpretation of some axial mesons as chiral partners for vector mesons. The $A_1(1260)$ has been seen as the chiral partner of the rho meson and the $f_1(1285)$ [1] meson is a candidate for the chiral partner for the ω . However the strict relation of phenomenological models describing their interactions to nucleons, and therefore to constituent quarks, to the more fundamental QCD degrees of freedom is not completely settled. There are several different approaches for describing vector mesons dynamics such as massive Yang Mills, hidden gauge approach, and others [2–6] that are not necessarily equivalent. However, a desirable incorporation of vector (and axial) mesons to the usual chiral perturbation theory framework, as an effective field theory, has found some difficulties [7,8]. The vector mesons couplings to nucleons have shown much fewer ambiguities since Sakurai's work [2,9,10]. There has been great interest in these couplings to describe finite baryonic densities hadron systems including at the saturation density [11,12]. The difficulty in determining the

hadron coupling constants values from first principles QCD has lead to different developments. At the purely quark level, instantons have been shown to provide effective quark interactions that should contribute for hadron structure. In Ref. [13] light vector (axial) mesons couplings to constituent quarks were derived by departing from a one loop quark polarization by making use of the auxiliary field method to introduce vector and axial mesons fields. In the present work the vector and axial mesons coupling to quarks are addressed in the presence of a weak background photon. Vector/axial mesons electrical charges couplings to the photon are recovered as well as some of the couplings associated to vector meson dominance.

Besides the interest in understanding the emergence of baryons and mesons couplings to the electromagnetic field in terms of the more fundamental quark and gluon degrees of freedom, recently it has been recognized that magnetic fields might generate several interesting effects in strongly interacting systems such as magnetic catalysis, CP violation, chiral magnetic effect, and others [14–22]. Their effects should be sizeable, in particular, in magnetars and peripheral heavy ion collisions [23]. Magnetic field effects might be larger for processes with enough energy to involve light vector and axial mesons than in the very low energy regime where pions are by far the most important degrees of freedom as the Goldstone bosons of DChSB. From the theoretical point of view it has been found that finite magnetic fields induce modifications in the quark, gluon, and hadron interactions [24–31]. In the present work, effective couplings of constituent quarks to light vector/axial mesons in the presence of a weak background magnetic field are derived from one loop quark polarization for dressed one gluon exchange quark-quark interaction.

The light vector and axial mesons are introduced by means of the usual auxiliary field method and they are identified with vector and axial quark currents such as $\bar{\psi}\gamma_\mu\sigma_i\psi$, $\bar{\psi}\gamma_\mu\psi$, and $\bar{\psi}\gamma_5\gamma_\mu\sigma_i\psi$, $\bar{\psi}\gamma_5\gamma_\mu\psi$. Eventual corrections by other types of Dirac structures are neglected. The specific vector and axial mesons sector, without the coupling to constituent quarks, that has been investigated by other groups in similar and complementary approaches [4,32], is outside the scope of the present work. This work is organized as follows. In the next section the approach is described in a succinct way since a more detailed explanation can be found in Refs. [29,33,34]. The quark determinant is expanded for large effective quark mass and weak external electromagnetic field. Effective coupling constants for simultaneous couplings of constituent quarks, vector/axial mesons, and the photon are resolved and expressed in terms of the parameters of the original model and of components of the quark and gluon propagators. In the following section a weak magnetic field is considered and the effective light vector mesons couplings to constituent quarks are rewritten to exhibit magnetic field dependent coupling constants. Numerical estimates for the hadrons effective coupling constants are presented as being highly dependent on the choice of the gluon propagator and on the particular values for the quark-gluon coupling constant. Some analytical simple ratios between the effective coupling constants are found to provide their approximated relative strengths in the limit of very large quark mass. Finally, the dependences of the rho meson electric form factor and its electromagnetic radius on the weak magnetic field are presented. A summary is presented in the final section.

II. QUARK POLARIZATION AND VECTOR MESONS

The one dressed gluon exchange quark-quark interaction is one of the leading terms of QCD effective action. By considering the minimal coupling to a background electromagnetic field, its generating functional is given by [35,36]

$$Z = N \int \mathcal{D}[\bar{\psi}, \psi] \exp i \int_x \left[\bar{\psi}(i\not{D} - m)\psi - \frac{g^2}{2} \int_y j_\mu^b(x) \tilde{R}_{bc}^{\mu\nu}(x-y) j_\nu^c(y) + \bar{\psi}J + J^*\psi \right], \quad (1)$$

where \int_x stands for $\int d^4x$, $i, j, k = 0, \dots, (N_f^2 - 1)$ is used for SU(2) flavor indices, and $a, b, \dots = 1, \dots, (N_c^2 - 1)$ stands for color in the adjoint representation. The color quark current is given by $j_a^\mu = \bar{\psi}\lambda_a\gamma^\mu\psi$, and the sums in color, flavor, and Dirac indices are implicit. $D_\mu = \partial_\mu\delta_{ij} - ieQ_{ij}A_\mu$ is the covariant quark derivative with the minimal coupling to photons, with the diagonal matrix $\hat{Q} = \text{diag}(2/3, -1/3)$. The gluon propagator, $\tilde{R}_{ab}^{\mu\nu}(x-y)$, must be a nonperturbative one, being an external input. This

makes it possible to incorporate to some extent the gluonic non-Abelian character. Besides that, it is required that this nonperturbative gluon kernel, eventually with a corrected quark-gluon coupling, provides enough strength to yield DChSB. This has been found in several approaches [37–41]. In several Landau-type gauges this kernel can be written in terms of transversal and longitudinal components, $R_T(x-y)$ and $R_L(x-y)$, as $\tilde{R}_{ab}^{\mu\nu}(x-y) \equiv \tilde{R}_{ab}^{\mu\nu} = \delta_{ab}[(g^{\mu\nu} - \frac{\partial^\mu\partial^\nu}{\partial^2})R_T(x-y) + \frac{\partial^\mu\partial^\nu}{\partial^2}R_L(x-y)]$.

The method employed in the present work was developed at length in Refs. [29,33,34], so it is shortly described here. First, a Fierz transformation [36,42,43] makes it possible to exploit the flavor structure of the interaction above. It can be written as $\Omega = \mathcal{F}(\frac{g^2}{2} j_\mu^b(x) \tilde{R}_{bc}^{\mu\nu}(x-y) j_\nu^c(y))$. The complete color singlet part of the Fierz transformed interaction is written in terms of the bilocal flavor-quark currents $j_q(x,y) = \bar{\psi}(x)\Gamma^q\psi(y)$, where $q = s, p, si, ps, v, a, vs, as$ denotes respectively the following operators for flavor and Dirac indices: $\Gamma_s = I_2 \cdot I_4$ (for the 2×2 flavor and 4×4 identities), $\Gamma_p = i\gamma_5\sigma_i$, $\Gamma_{si} = \sigma_i \cdot I_4$, $\Gamma_{ps} = i\gamma_5 I_2$, $\Gamma_v = \gamma^\mu\sigma_i$, $\Gamma_a = \gamma_5\gamma^\mu\sigma_i$, $\Gamma_{vs} = \gamma^\mu$, and $\Gamma_{as} = \gamma_5\gamma^\mu$, σ_i being the flavor SU(2) Pauli matrices. The complete set of resulting color singlet nonlocal interactions is as follows:

$$\frac{\Omega}{\alpha g^2} \equiv [j_S(x,y)j_S(y,x) + j_P^i(x,y)j_P^i(y,x) + j_P(x,y)j_P(y,x)]R_{(x-y)} - \frac{1}{2}[j_\mu^i(x,y)j_\nu^i(y,x) + j_{\mu A}^i(x,y)j_{\nu A}^i(y,x) + j_\mu(x,y)j_\nu(y,x) + j_\mu^A(x,y)j_\nu^A(y,x)]\tilde{R}_{(x-y)}, \quad (2)$$

where $\alpha = 4/9$ for SU(2) flavor. The kernels above can be written as

$$R(x-y) \equiv R = 3R_T(x-y) + R_L(x-y), \\ \tilde{R}^{\mu\nu}(x-y) \equiv \tilde{R}^{\mu\nu} = g^{\mu\nu}(R_T(x-y) + R_L(x-y)) + 2\frac{\partial^\mu\partial^\nu}{\partial^2}(R_T(x-y) - R_L(x-y)). \quad (3)$$

The background field method (BFM) [44] is applied next by splitting the quark field into quarks composing quark-antiquark states including the chiral condensate, ψ_2 , and the background constituent quark, ψ_1 . At the one loop level it is enough to perform the shift of quark bilinears such as $\bar{\psi}\Gamma^q\psi \rightarrow (\bar{\psi}\Gamma^q\psi)_2 + (\bar{\psi}\Gamma^q\psi)_1$. This splitting preserves chiral symmetry and it is not associated to a simple mode separation of low and high energies since this may be a restrictive assumption. The effective interaction Ω is then rewritten as $\Omega = \Omega_1 + \Omega_2 + \Omega_{12}$. When Ω_2 is neglected it yields the usual one loop BFM. However it is possible to improve that by considering the auxiliary field method to

introduce quark-antiquark light mesons and to incorporate the DChSB with a large constituent quark effective mass in the lines of the Nambu-Jona-Lasinio (NJL) model [29,30,33,34]. The following set of bilocal auxiliary fields (a.f.) is introduced by means of unitary functional integrals multiplying the generating functional: $S(x, y), P_i(x, y),$

$S_i(x, y), P(x, y), V_\mu^i(x, y), V_\mu(x, y), \bar{A}_\mu^i(x, y),$ and $\bar{A}_\mu(x, y)$. Each of these fields corresponds to a specific channel Γ_q of the color singlet Fierz transformed interaction Ω above. The following normalized Gaussian integrals multiply the generating functional:

$$\begin{aligned}
 1 &= N \int D[S]D[P_i]D[S_i]D[P]e^{-\frac{i}{2} \int_{x,y} R\alpha[(S-gJ_{i(2)}^S)^2+(P_i-gJ_{i(2)}^P)^2]+[(S_i-gJ_{i(2)}^S)^2+(P-gJ_{(2)}^P)^2]} \\
 &\times \int D[V_\mu^i] \int D[\bar{A}_\mu^i]e^{-\frac{i}{4} \int_{x,y} \bar{R}^{\mu\nu}\alpha[(V_\mu^i-gJ_{V,\mu}^{i(2)})(V_\nu^i-gJ_{V,\nu}^{i(2)})]}e^{-\frac{i}{4} \int_{x,y} \bar{R}^{\mu\nu}\alpha[(\bar{A}_\mu^i-gJ_\mu^{i(2)A})(\bar{A}_\nu^i-gJ_\nu^{i(2)A})]} \\
 &\times \int D[V_\mu] \int D[\bar{A}_\mu]e^{-\frac{i}{4} \int_{x,y} \bar{R}^{\mu\nu}\alpha[(V_\mu-gJ_{V,\mu}^{(2)})(V_\nu-gJ_{V,\nu}^{(2)})]}e^{-\frac{i}{4} \int_{x,y} \bar{R}^{\mu\nu}\alpha[(\bar{A}_\mu-gJ_\mu^{(2)A})(\bar{A}_\nu-gJ_\nu^{(2)A})]}. \quad (4)
 \end{aligned}$$

In these integrals there are shifts of each of the auxiliary fields that provide interactions that cancel out completely the interaction Ω_2 . All these shifts yield unity Jacobian. The structureless meson field limit can be reached by expanding the bilocal auxiliary fields in an infinite basis of local fields and by keeping only the lowest energy states modes [35]. This yields the local limit interactions for punctual light mesons. The scalar-pseudoscalar sector has been considered extensively within this approach in Refs. [30,33,35,36] and it is neglected from here on, except for the fact that scalar auxiliary fields generate the quark effective mass. The specific vector/axial mesons couplings to the valence quarks reduce to

$$\begin{aligned}
 &\bar{\psi}_2(x)\Xi_v(x, y)\psi_2(y) \\
 &\simeq -\bar{\psi}_2(x)\frac{\gamma^\mu}{2}[F_v\sigma_i(V_\mu^i(x) + \gamma_5\bar{A}_\mu^i(x)) \\
 &\quad + F_{vs}(V^\mu(x) + \gamma_5\bar{A}^\mu(x))]\delta(x-y)\psi_2(y), \quad (5)
 \end{aligned}$$

where F_v, F_{vs} produce the correct canonical normalization of the vector/axial mesons field, $\phi_q' = F_q\phi_q$ for each of the channels q , respectively for rho and A_1 mesons and for ω and the axial isosinglet f_1 as chiral partners.

By performing a Gaussian integration of the valence quark field, the resulting determinant can be written, by means of the identity $\det A = \exp \text{Tr} \ln(A)$, as

$$S_{\text{eff}} = \text{Tr} \ln \{-iS_{c,q}^{-1}(x-y)\}, \quad (6)$$

$$\begin{aligned}
 S_{c,q}^{-1}(x-y) &\equiv S_{0,c}^{-1}(x-y) + \Xi_s(x-y) + \sum_q a_q \Gamma_q J_q(x, y) \\
 &= S_c^{-1}(x-y) + \sum_q a_q \Gamma_q J_q(x, y), \quad (7)
 \end{aligned}$$

where Tr stands for traces of all discrete internal indices and integration of spacetime coordinates and $\Xi_s(x-y)$ stands for the coupling of valence quark to the scalar-pseudoscalar

fields presented in [30,33]. Their only contribution emerges for the quark effective mass due to the DChSB. The quark kernel can be written as $S_{0,c}^{-1}(x-y) = (i\not{D} - m)\delta(x-y) + \Xi_v(x-y)$, where m is so far the current quark mass. In expression (7) the following quantity with all the constituent quark currents has been used:

$$\begin{aligned}
 &\frac{\sum_q a_q \Gamma_q J_q(x, y)}{\alpha g^2} \\
 &= 2R(x-y)[\bar{\psi}(y)\psi(x) + i\gamma_5\sigma_i\bar{\psi}(y)i\gamma_5\sigma_i\psi(x) \\
 &\quad + \bar{\psi}(y)\sigma_i\psi(x) + i\gamma_5\bar{\psi}(y)i\gamma_5\psi(x)] \\
 &\quad - \bar{R}^{\mu\nu}(x-y)\gamma_\mu\sigma_i[\bar{\psi}(y)\gamma_\nu\sigma_i\psi(x) + \gamma_5\bar{\psi}(y)\gamma_5\gamma_\nu\sigma_i\psi(x)] \\
 &\quad - \bar{R}^{\mu\nu}(x-y)\gamma_\mu[\bar{\psi}(y)\gamma_\nu\psi(x) + \gamma_5\bar{\psi}(y)\gamma_5\gamma_\nu\psi(x)]. \quad (8)
 \end{aligned}$$

The absence of a tensor current $\bar{\psi}\sigma_{\mu\nu}\psi$ goes back to the Fierz transformed quark-quark interaction above. Although this tensor structure might also contribute to vector mesons structure and interactions [45]. However the mechanism by which it is generated, as well as the tensor couplings to vector mesons and photons, is not the one addressed in the present work. The auxiliary fields are undetermined so far and the saddle point equations for expression (6), with the remaining Lagrangian terms from the introduction of the auxiliary fields, yield usual gap equations. By denoting each of the eight meson fields as ϕ_q for the channel q , the gap equations are obtained from the corresponding saddle point equations, $\frac{\partial S_{\text{eff}}}{\partial \phi_q} = 0$. These equations for the NJL model and for the model (1) have been analyzed in many works in the vacuum or under a finite energy density, in particular, in the presence of a finite external magnetic field, $A_\mu = B_0(0, 0, x, 0)$. At zero magnetic field the scalar auxiliary field is the only one that can be different from 0 in the vacuum and indeed its nontrivial solution for a gluon kernel with enough strength in the infrared regime has been extensively investigated. The resulting scalar mean field corresponds to the quark-antiquark condensate whose value

is strongly dependent on the magnetic field. At zero temperature, magnetic catalysis can increase considerably quark effective mass. These contributions are incorporated into the quark kernel (7) by defining the quark effective mass. The redefined quark kernel can be written as

$$S_{0,c}^{-1}(x-y) = (i\not{D} - M^*)\delta(x-y) + \Xi_v(x-y). \quad (9)$$

This kernel, and therefore the gap equations, are B_0 dependent and the resulting values for the effective quark mass $M^*(B_0)$ are considered in the numerical estimations in Sec. III A. Below only the constituent quark and vector/axial mesons are considered.

A. Expansion of the determinant

From expression (6) the quark kernel coupled to the photon and vector mesons fields can be factorized. It gives origin to a term of the type $I_V = \frac{1}{2}\text{Tr}(\tilde{S}_{0,c}^{-1}S_{0,c}^{-1})$. This term contains all the terms exclusively with vector mesons and photon fields including corrections to the photon effective action. These terms lead to an effective action of the type of the celebrated Euler Heisenberg effective action [46–48]. In Ref. [4] the chiral vector mesons sector (ρ and A_1), without quarks and photon fields, was investigated. These two sectors are not addressed in the present paper. Other limits of this determinant were investigated for example in [29,34] where respectively constituent quark effective interactions were presented considering higher order terms and magnetic field dependent corrections to the usual NJL and vector-NJL interactions. In [13] a set of constituent quark-vector/axial mesons couplings has been presented and the emergence of gauge-type vector mesons couplings to constituent quarks were found along the lines of the Sakurai proposal [2]. Below only effective couplings of the photon field to constituent quarks and vector/axial mesons are addressed. For this, the mesons fields and the constituent quark component are treated as background fields.

The leading terms in the very long-wavelength local limit for zero momentum transfer are the following:

$$I_{AV} = g_{qA} \left(A_\mu(x) j_3^\mu(x) + \frac{1}{3} A_\mu(x) j^\mu(x) \right), \quad (10)$$

where the effective coupling constant was resolved by calculating the traces in color, Dirac and isospin indices,

$$g_{qA} = -i4N_c d_1 e \times (\alpha g^2) \text{Tr}'((S_0(k)S_0(k)\bar{R}(k))), \quad (11)$$

where $d_n = (-1)^{n+1}/(2n)$, Tr' stands for momentum integration, $S_0^{-1}(k) = (k - M^*)$ by implicitly assuming regularization procedure, and $\bar{R}(k) = \bar{R}^{\mu\nu}(k)g_{\mu\nu}$. The double parenthesis denotes the integration for the zero momentum limit of the corresponding form factor. These photon-constituent quark couplings can be associated to

vector meson dominances for the neutral mesons ρ^0 and ω . The factor $1/3$ is the usual one in quark models; see for example [49].

By considering the canonical definition of all the vector and axial mesons, four types of photon-vector/axial meson-constituent quark emerge. The leading terms for each of them, in the long-wavelength local limit with zero momentum transfer and by omitting the spacetime dependence of the mesons and photon fields and quark currents, are given by

$$I_{FF} = 2g_1 i\epsilon_{ij3} (F_{\mu\nu} \mathcal{G}_i^{\mu\nu} j_p^j + F_{\mu\nu} \mathcal{F}_i^{\mu\nu} j_s^j), \quad (12)$$

$$I_{FFm} = g_1 [F_{\mu\nu} \mathcal{F}_3^{\mu\nu} j_s + F_{\mu\nu} \mathcal{F}^{\mu\nu} j_s^3 + F_{\mu\nu} \mathcal{G}_3^{\mu\nu} j_p + F_{\mu\nu} \mathcal{G}^{\mu\nu} j_p^3 + \frac{1}{3} (F_{\mu\nu} \mathcal{G}^{\mu\nu} j_p + F_{\mu\nu} \mathcal{F}^{\mu\nu} j_s + F_{\mu\nu} \mathcal{G}_i^{\mu\nu} j_p^i + F_{\mu\nu} \mathcal{F}_i^{\mu\nu} j_s^i)], \quad (13)$$

$$I_{VA} = 2g_2 i\epsilon_{ij3} (A_\rho V_i^\rho j_s^j + A_\rho \bar{A}_i^\rho j_p^j), \quad (14)$$

$$I_{VAm} = g_2 \left[A^\rho \bar{A}_\rho^3 j_p + A^\mu \bar{A}_\mu j_p^3 + A^\nu V_\nu^3 j_s + A^\nu V_\nu j_s^3 + \frac{1}{3} (A^\nu V_\nu j_s + A^\mu \bar{A}_\mu j_p + A_\rho V_i^\rho j_s^i + A^\mu \bar{A}_\mu^i j_p^i) \right], \quad (15)$$

$$I_{VF} = g_3 i\epsilon_{ij3} (F_{\rho\delta} V_i^\rho j_{j,V}^\delta + F_{\rho\delta} \bar{A}_i^\rho j_{j,A}^\delta), \quad (16)$$

$$I_{AF} = g_3 i\epsilon_{ij3} (\mathcal{F}_{\rho\delta}^i A^\rho j_{j,V}^\delta + \mathcal{G}_{\rho\delta}^i A^\rho j_{j,A}^\delta), \quad (17)$$

where the following effective coupling constants have been defined as a zero momentum limit of their corresponding form factors,

$$g_1 = -i6M^* N_c d_1 e (\alpha g^2) \text{Tr}'((\tilde{S}_0(k)\tilde{S}_0(k)\tilde{S}_0(k)R(k))), \quad (18)$$

$$g_2 = -i6M^* N_c d_1 e (\alpha g^2) \text{Tr}'((\tilde{S}_0(k)\tilde{S}_0(k)R(k))), \quad (19)$$

$$g_3 = M^* g_1, \quad (20)$$

where it was defined $\tilde{S}_0 = \frac{1}{k^2 - M^{*2}}$. The couplings I_{FF} , I_{VA} , I_{VF} , and I_{AF} are the leading photon couplings to vector and axial and corresponding constituent quark currents by their resulting electrical charges. The effective couplings I_{FFm} and I_{VAm} describe different channels of mixing interactions (or vector meson dominances) induced or mediated by constituent quark currents. In a first analysis, in the large effective mass limit, the effective couplings in I_{VA} and I_{VAm} (with g_2) might be seen as the leading ones. However, it is shown in the next section that this might not happen depending on the electromagnetic field configuration. For a weak magnetic field it becomes of the same order as the leading dipolar couplings I_{FF} and I_{FFm} (with g_1). These

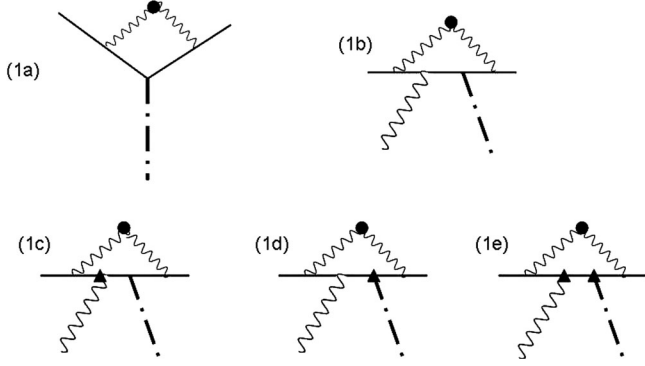


FIG. 1. In these diagrams, the wavy line with a full dot is a (dressed) nonperturbative gluon propagator, a solid line represents a constituent quark, the single wavy line stands for a photon, the wavy line with a triangle in the vertex corresponds to the photon strength tensor $F^{\mu\nu}$, the dashed-dotted line represents a vector or axial meson V_μ^α , and the dashed-dotted line with a triangle in the vertex stands for the Abelian strength tensor $\mathcal{F}_{\mu\nu}^\alpha$ of a vector or axial meson α .

photon couplings break chiral and isospin symmetry as expected.

The Feynman diagrams for these effective couplings are shown in Fig. 1. Diagram (1a) can be seen as a vector meson dominance process from expression (10); diagrams (1b)–(1e) correspond to the effective interactions of expressions (12)–(17). They are rather related to the zero momentum limit of vector meson photoproduction; however they can also be seen as vector meson dominances or mixings mediated or induced by a corresponding constituent quark current.

III. WEAK MAGNETIC FIELD DEPENDENT EFFECTIVE COUPLINGS

By considering a weak magnetic field along the \hat{z} direction, with $A^\mu = (0, 0, B_0 x, 0)$, it can be effectively incorporated in the meson-quark coupling constants. For that, some of the expressions above must be recalculated. From expression (10) the free quark vector current receives the following asymmetric term from the coupling to the magnetic field:

$$I_{AV} = ig_{qA}^B \left(j_3^y + \frac{1}{3} j^y \right), \quad (21)$$

where the following leading contribution to the effective parameter was defined,

$$g_{qA}^B = -i4N_c d_1 (eB_0) \alpha g^2 \text{Tr}' \left(\left(-\frac{\partial}{\partial k_x} \tilde{S}_2(k) \bar{R}(k) \right) \right), \quad (22)$$

being however trivially 0 due to rotational invariance for this zero momentum exchange limit.

TABLE I. In the first column the values considered for the quark effective mass are displayed; in the second column the values for the magnetic field in terms of the quark effective mass and of the pion mass ($\frac{eB_0}{M^{*2}}, \frac{eB_0}{m_\pi^2}$) are displayed. The gluon propagator is indicated in the next column: D_I and D_{II} are the gluon propagators respectively from Refs. [37,38] and Ref. [40]. In the fourth column the gauge-type vector/axial meson couplings to quark currents are presented from Ref. [13]. In the fifth and sixth columns, results from the expressions (19) and (31) are the second one divided by factor $(eB_0)/M^{*2}$.

M^* (GeV)	$(\frac{eB_0}{M^{*2}}, \frac{eB_0}{m_\pi^2})$	$D_i(k)$...	g_{r1} ...	g_2 (GeV ⁻¹)	$g_3^{B_1} / (\frac{eB_0}{M^{*2}})$...
0.33	(0, 0)	D_I	9.3	5.6	1.7
0.38	(0.2, 1.5)	D_I	8.2	4.7	1.8
0.45	(0.5, 5.2)	D_I	6.8	3.6	1.8
0.33	(0, 0)	D_{II}	1.1	0.3	0.19
0.38	(0.2, 1.5)	D_{II}	0.9	0.3	0.19
0.45	(0.5, 5.2)	D_{II}	0.8	0.2	0.19
0.22	(0, 0)	D_I	12.7	8.6	1.4
0.25	(0.2, 0.6)	D_I	11.6	7.7	1.6
0.28	(0.5, 2)	D_I	10.7	6.8	1.6
0.22	(0, 0)	D_{II}	1.5	0.6	0.19
0.25	(0.2, 0.6)	D_{II}	1.3	0.5	0.19
0.28	(0.5, 2)	D_{II}	1.2	0.4	0.19
0.07	(0, 0)	D_I	20.3	14.7	0.5
0.085	(0.2, .08)	D_I	19.4	14.0	0.6
0.10	(0.5, 0.3)	D_I	18.5	13.3	0.7
0.07	(0, 0)	D_{II}	2.4	0.9	0.06
0.085	(0.2, .08)	D_{II}	2.3	0.9	0.08
0.10	(0.5, 0.3)	D_{II}	2.1	0.9	0.1

For the leading photon vector or axial meson and constituent quark effective interactions (12)–(17) the following B_0 -dependent anisotropic vector meson-constituent quark couplings emerge,

$$I_{FF} \rightarrow 2g_1^B i\epsilon_{ij3} [\mathcal{G}_i^{xy} j_p^j + \mathcal{F}_i^{xy} j_s^j], \quad (23)$$

$$I_{FFm} \rightarrow g_1^B \left[\mathcal{F}_3^{xy} j_s^3 + \mathcal{F}^{xy} j_s^3 + \mathcal{G}_3^{xy} j_p^3 + \mathcal{G}^{\mu\nu} j_p^3 + \frac{1}{3} (\mathcal{G}^{xy} j_p^3 + \mathcal{F}^{xy} j_s^3 + \mathcal{G}_i^{xy} j_p^i + \mathcal{F}_i^{xy} j_s^i) \right], \quad (24)$$

$$I_{VA} \rightarrow 2g_2^B i\epsilon_{ij3} [\bar{A}_i^y j_p^j + V_i^y j_s^j], \quad (25)$$

$$I_{VAm} \rightarrow g_2^B \left[\bar{A}_y^3 j_p^3 + \bar{A}_y j_p^3 + V_y^3 j_s^3 + V_y j_s^3 + \frac{1}{3} (V_y j_s^3 + \bar{A}_y j_p^3 + V_y^i j_s^i + \bar{A}_y^i j_p^i) \right], \quad (26)$$

$$I_{VF} \rightarrow g_3^{B_1} i\epsilon_{ij3} [V_i^x j_{j,V}^y + \bar{A}_i^x j_{j,A}^y], \quad (27)$$

$$I_{AF} \rightarrow g_3^{B_2} i\epsilon_{ij3} [\mathcal{F}_{y\delta}^i j_{j,V}^\delta + \mathcal{G}_{y\delta}^i j_{j,A}^\delta], \quad (28)$$

where the following effective coupling constants have been defined in the long-wavelength limit for zero momentum transfer:

$$g_1^B = -i6M^*N_c d_1(eB_0)(\alpha g^2) \text{Tr}'((\tilde{S}_0(k)\tilde{S}_0(k)\tilde{S}_0(k)R(k))), \quad (29)$$

$$g_2^B = -i6M^*N_c d_1(eB_0)(\alpha g^2) \text{Tr}'\left(\left(-\tilde{S}_0(k)R(k)\frac{\partial}{\partial k_x}\tilde{S}_0(k)\right)\right), \quad (30)$$

$$g_3^{B_1} = i6M^{*2}N_c d_1(eB_0)(\alpha g^2) \text{Tr}'((\tilde{S}_0(k)\tilde{S}_0(k)\tilde{S}_0(k)R(k))), \quad (31)$$

$$g_3^{B_2} = i6M^{*2}N_c d_1(eB_0)(\alpha g^2) \times \text{Tr}'\left(\left(-\tilde{S}_0(k)\tilde{S}_0(k)R(k)\frac{\partial}{\partial k_x}\tilde{S}_0(k)\right)\right). \quad (32)$$

The coupling constants g_2^B and $g_3^{B_2}$ are 0 in the zero momentum transfer limit due to rotational invariance. The couplings with $g_3^{B_1}$, $g_3^{B_2}$ are momentum independent and dependent anisotropic corrections to the gauge-type coupling. These corrections arise in the plane orthogonal to the magnetic field, and this can be more conveniently written for a magnetic field given by $A_\mu = (0, -y, x, 0)B_0/2$. This magnetic field makes explicit the equivalence between the orthogonal components x and y . These effective coupling constants do not have all the same dimensions; however some approximated or exact ratios in the limit of very large quark effective mass can be obtained such as

$$\frac{g_1^B}{g_3^{B_1}} \sim \frac{1}{M^*}, \quad \frac{g_3^{B_2}}{g_2^B} = \frac{1}{M^*}. \quad (33)$$

The second of these ratios has a gauge invariant form. The largest strengths of the corrections to the vector meson-constituent quarks effective couplings due to a weak magnetic field appear in the channels I_{FF} , I_{VA} , and I_{VF} , being the first and the third dipolar photon couplings.

It is interesting to compare these magnetic field dependent couplings constants with the corresponding gauge-type coupling constants of vector and axial mesons to constituent quarks in the vacuum as presented in Ref. [13]. Consider expressions (14) and (15) of [13] written in terms of the canonically defined vector fields given by

$$L_{v-q} = g_{r1}(V_i^\mu(x)j_\mu^{V,i}(x) + \bar{A}_i^\mu(x)j_\mu^{A,i}(x)) + g_{v1}(V^\mu(x)j_\mu(x) + \bar{A}_\mu(x)j_A^\mu(x)), \quad (34)$$

where the dimensionless coupling constants were found to be

$$g_{r1} = g_{v1} = 4id_1N_c(\alpha g^2) \text{Tr}'((\tilde{S}_0(k)S_0(k)\bar{R}(k))). \quad (35)$$

A simple comparison with expression (11) yields a relation with the electromagnetic coupling, $2g_{qA} = eg_{r1}$. An approximated estimate of the relative strength of the weak B_0 -induced anisotropic correction to charged vector mesons gauge-type coupling can be written as

$$\frac{g_3^{B_1}}{g_{r1}} \sim \frac{3eB_0}{4M^{*2}}. \quad (36)$$

A. Numerical estimations and form factors

In the table below numerical values for the effective coupling constants $g_3^{B_1}$ and g_2 , expressions (31) and (19), are shown respectively in the fifth and sixth columns and compared to the resulting values of the gauge-type coupling g_{r1} from Ref. [13]—in the fourth column of the table. The quark effective mass dependence on the weak magnetic field was taken into account and different values are shown in the first column of the table: values at zero magnetic field, $M^*(B_0 = 0) = 0.33, 0.22, \text{ and } 0.07$ GeV, and the corresponding values for a given magnetic field in the second column, $(eB_0)/M^{*2}$ and also $(eB_0)/m_\pi^2$, where m_π^2 is the squared pion mass in the vacuum (140 MeV). For $eB_0 \approx 5m_\pi^2 \approx 10^{18}$ G being therefore expected to be sizeable in magnetars and eventually in heavy ion collisions [23]. For not so small parameters $eB_0/M^{*2} \geq 0.5$ other types of couplings might be expected to appear and the strength of the effective couplings shown in the table might receive further corrections. Two very different nonperturbative gluon propagators were chosen to make clear the ambiguity of the numerical estimates when calculating the momentum integrals of the expressions above. These integrations were carried out after a Wick rotation to Euclidean momentum space. The first of the gluon propagators, $D_I(k)$, is a transversal component one from Tandy-Maris [37,38] and the second one, $D_{II}(k)$, is an effective longitudinal one by Cornwall [40] that also produces dynamical chiral symmetry breaking. They are indicated in the third column of the table. The following convention was adopted: $g^2\tilde{R}^{\mu\nu}(k) \equiv D_i^{\mu\nu}(k)$ where $i = I, II$. The values of anisotropic correction to the gauge-type coupling constant $g_3^{B_1}$ were divided by $(eB_0)/M^{*2}$ in such a way to depend on the magnetic field only by means of the quark effective mass. Therefore the values in the table must be multiplied by $(eB_0)/M^{*2}$ to yield their contributions to the couplings. For the sake of comparison, the corresponding values for the gauge-type coupling constant of vector mesons to constituent quarks are included in the fourth column extracted from Ref. [13]. In spite of the different values due to the different gluon propagators and quark-gluon coupling constants they have basically the same order of magnitude of the usual vector and omega mesons to nucleons [50]. All the results show the direct dependence on the gluon propagator and on the strength of the quark-gluon

coupling g^2 . It should be noted that the complete expression for the momentum dependent effective couplings such as g_1 and g_3 for I_{FF} , I_{FFm} , and I_{AF} must be considered as multiplied by the external vector meson momentum Q .

The complete momentum dependent expression for g_{qA} in (10) turns out to be the leading electric form factor for the vector mesons,

$$g_{qA}(Q) = F_1^\rho(Q) = 3F_1^\omega(Q). \quad (37)$$

A leading anisotropic correction due to the weak magnetic field is obtained from I_{VF} in (27) so that for the case of the rho meson,

$$\Delta_B F_1^\rho(Q) = \frac{2}{3} g_3^{B_1}(Q). \quad (38)$$

The expressions for the form factors g_{qA} and $g_3^{B_1}$, respectively from expressions (11) and (31), can be written for nonzero momentum transfer as

$$g_{qA}(Q) = 8eN_c d_1 K_0 \int_q S_0(q) S_0(q+Q) R(-q), \quad (39)$$

$$\frac{g_3^{B_1}(Q)}{(eB_0/M^{*2})} = 6N_c d_1 K_0 M^{*4} \int_q \tilde{S}_0(q) \tilde{S}_0^2(q+Q) R(-q). \quad (40)$$

In Figs. 2 and 3 these form factors respectively for the propagator $D_I(k)$ [37,38] and $D_{II}(k)$ [40] are compared to the vector-meson-nucleon form factor calculated in Ref. [51] by considering the Faddeev equation. This last form factor was interpolated by the following quadrupole shape [51]: $F_1^\rho(Q^2) = \frac{F_1^\rho(0)}{(1 + \frac{Q^2}{\Lambda_{1,\rho}^2})^3}$, where $\Lambda_{1,\rho} = 1.12$ GeV,

where $F_1^\rho(0) = g_{\rho NN}$ is in the range 4.82–6.4 in different works. To allow the comparison of the strict momentum dependence of the form factors the value of $F_1^V(0) = 5$ was multiplied by a numerical factor to coincide with the numerical zero momentum form factors obtained in this work. Therefore in Fig. 2 $F_1^\rho(0) = 2.8$ and in Fig. 3 $F_1^\rho(0) = 0.21$.

The rho meson quadratic charge radius with an anisotropic correction due to the weak magnetic field is also calculated. It can be written as

$$\begin{aligned} \langle r_\rho^2 \rangle(B_0) &= -6 \frac{dF_{1,\rho}^E(Q^2)}{dQ^2} \Big|_{Q=0} \\ &= -6 \frac{d}{dQ^2} \left(g_{qA}(Q) + \frac{2}{3} g_3^{B_1}(Q) \right) \Big|_{Q=0} \\ &\equiv \langle r_\rho^2(M^*) \rangle + \frac{eB_0}{M^{*2}} \Delta \langle r_\rho^2(M^*) \rangle. \end{aligned} \quad (41)$$

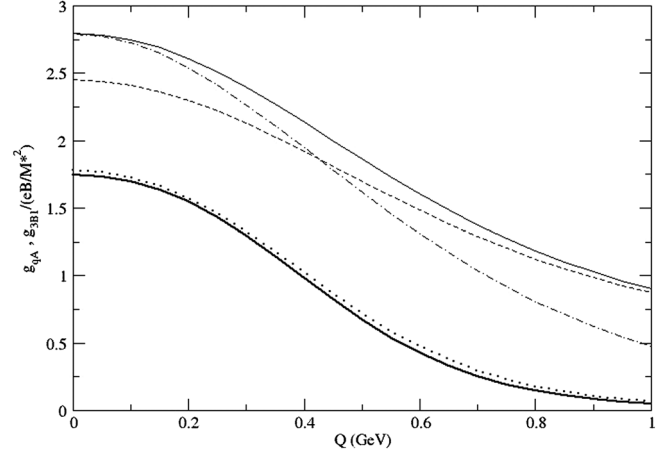


FIG. 2. The form factors $g_{qA}(Q)$ and $g_3^{B_1}(Q)$ from expressions (39) and (40) are shown for the gluon propagator $D_I(k)$ of Refs. [37,38]. The thin solid line stands for $g_{qA}(Q)$ with $M^* = 330$ MeV (for $B_0 = 0$) and the dashed line for $M^* = 380$ MeV, i.e., it corresponds to an effective mass at $eB_0 = 0.2M^{*2}$. The thick solid line represents the anisotropic correction $g_3^{B_1}(Q)$ for $M^* = 330$ MeV whereas the dotted line stands for $M^* = 380$ MeV for $eB_0 = 0.2M^{*2}$. To add the anisotropic correction to the form factor g_{qA} it still must be multiplied by $(eB_0)/M^{*2}$. The quadrupole fit of the rho meson-nucleon electric form factor from Ref. [51] is shown in the dotted-dashed line for $F_1^V(0) = 2.8$.

Numerical estimates are presented in Figs. 3 and 4 as functions of eB_0/M^{*2} respectively for the gluon propagators of Refs. [37,38,40] for $M^*(B_0 = 0) = 330$ MeV. In these figures the symbol \times indicates the leading correction

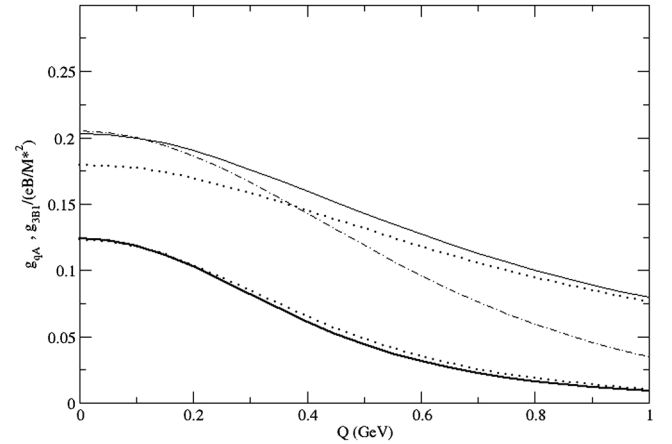


FIG. 3. The form factors $g_{qA}(Q)$ and $g_3^{B_1}(Q)$ from expressions (39) and (40) are shown for the gluon propagator $D_{II}(k)$ of Ref. [40]. The thin solid line $g_{qA}(Q)$ stands for $M^* = 330$ MeV (for $B_0 = 0$) and the dashed line for $M^* = 380$ MeV for $eB_0 = 0.2M^{*2}$. The thick solid line represents the anisotropic correction $g_3^{B_1}(Q)$ for $M^* = 330$ MeV whereas the dotted line stands for $M^* = 380$ MeV, i.e., it corresponds to an effective mass at $eB_0 = 0.2M^{*2}$. To add the anisotropic correction to the form factor g_{qA} it must be multiplied by $(eB_0)/M^{*2}$. The quadrupole fit of the rho meson-nucleon electric form factor from Ref. [51] is shown in the dotted-dashed line for $F_1^V(0) = 0.21$.

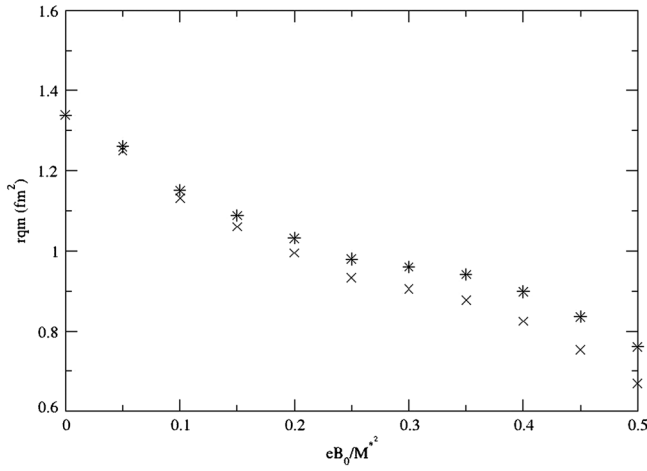


FIG. 4. The rho squared electromagnetic radius (rqm) with the gluon propagator $D_I(k)$ from Refs. [37,38] for $M^*(B_0 = 0) = 330$ MeV is shown as a function of the magnetic field in terms of the effective mass $(eB_0)/M^{*2}$. The symbol \times indicates the leading correction $\langle r_\rho^2(M^*) \rangle = -6 \frac{d}{dQ^2} g_{qA}(Q)$ in expression (41) and the symbols $*$ represent the total values of $\langle r_\rho^2 \rangle(B_0)$ with the anisotropic correction $(eB_0)/M^{*2}$.

$\langle r_\rho^2(M^*) \rangle = -6 \frac{d}{dQ^2} g_{qA}(Q)$ and the symbol $*$ represents the total values of $\langle r_\rho^2 \rangle(B_0)$ shown in expression (41). The large variation of $\langle r_\rho^2 \rangle(B_0)$ is exclusively due to the variation of the magnetic field quark effective mass. The anisotropic contribution $\Delta \langle r_\rho^2(M^*) \rangle$ is already multiplied by $(eB_0)/M^{*2}$ as indicated in expression (41). The discrepancies between the values obtained with the two different gluon propagators are of the same order of magnitude as those presented in the table. The experimental values are in the range of $0.28 \rightarrow 0.56$ fm² from Refs. [52,53].

IV. FINAL REMARKS

In this work the leading simultaneous photon effective couplings to light quark-antiquark vector/ axial mesons and to constituent quarks were derived by departing from the model given by (1) with QCD degrees of freedom. With these couplings, that can also be associated to the zero momentum limit of vector/axial mesons photoproduction form factors, it was possible to define weak magnetic field dependent constituent quarks couplings to vector/axial mesons as corrections to gauge-type mesons couplings to constituent quarks found in [13]. The leading terms in expression (10) for the photon-constituent quarks coupling correspond to vector meson dominance with a relative factor 1/3 for the omega vector meson. Concerning specifically the vector mesons-constituent quark simultaneous couplings to the photon, all the possible structures and channels that do not depend on tensor quark currents, but only on the currents considered, emerged in expressions (12)–(17). Some of the terms present a simple electrical charge coupling of the charged vector and axial mesons and

corresponding quark currents to the photon, and others exhibit the structure of vector meson dominance due to the interaction with a constituent quark current. All the effective coupling constants were expressed in terms of the parameters of the original Lagrangian (1) and components of quark and nonperturbative gluon propagators. The resulting effective couplings correspond to different channels and they break chiral and isospin symmetries as expected. The effective coupling constants are proportional to some power of the quark effective mass and therefore they disappear in the chiral limit with the restoration of chiral symmetry. Numerical estimates were presented and they exhibit the uncertainty in the knowledge of the gluon propagator and in the quark gluon (running) coupling constant at a particular energy scale. This can be noted in Table I and the discrepancies due to the used gluon propagator are also noted in Figs. 2–5. Although an external magnetic field has also been found to contribute to the gluon propagator and gluon coupling to quarks [24–28,54], these corrections were not considered in the present work. Besides the numerical estimates, approximated and exact ratios between the effective couplings were also calculated in the limit of large quark effective mass. These ratios yield the relative order of magnitude. Two form factors were also presented up to $Q = 1$ GeV: the rho electric form factor $F_1^V \propto g_{qA}$ and an anisotropic correction due to the weak magnetic field $\Delta F_a^V \propto g_3^{B1}$. The anisotropic contribution goes to 0 considerably faster than the form factor itself as seen in Figs. 2 and 3. Finally the corresponding rho electromagnetic radius with an anisotropic correction was also presented in Figs. 4 and 5 for

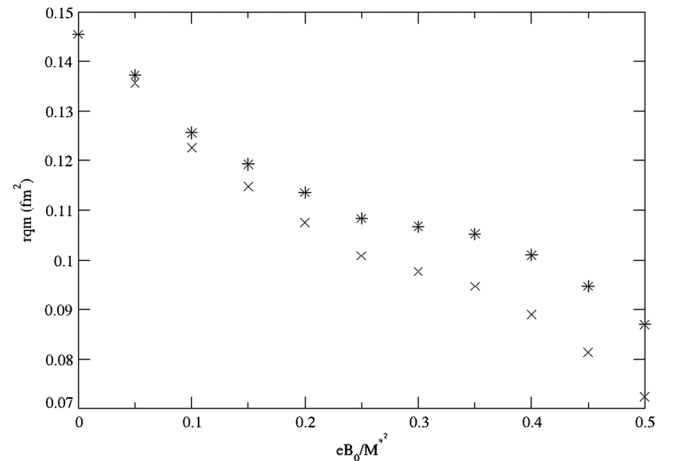


FIG. 5. The rho squared electromagnetic radius (rqm) with the gluon propagator $D_{II}(k)$ from Ref. [40] for $M^*(B_0 = 0) = 330$ MeV is shown as a function of the magnetic field in terms of the effective mass $(eB_0)/M^{*2}$. The symbol \times indicates the leading correction $\langle r_\rho^2(M^*) \rangle = -6 \frac{d}{dQ^2} g_{qA}(Q)$ in expression (41) and the symbols $*$ represent the total values of $\langle r_\rho^2 \rangle(B_0)$ with the anisotropic correction $(eB_0)/M^{*2}$.

both gluon propagators. The B_0 -dependent correction $g_3^{B_1}$ appears in the plane orthogonal to the weak magnetic field (\hat{k}). The most relevant contribution for the variation of both, the leading contribution for $\langle r_\rho^2 \rangle$ and the anisotropic correction, is due to the variation of the B_0 dependence of the quark effective mass. The anisotropic correction due to the coupling $g_3^{B_1}$ in Figs. 4 and 5 is considerably smaller but not negligible for $eB_0/M^{*2} \geq 0.3$. Higher order terms of the expansion in powers of the electromagnetic field were shown to provide a complete resummation for the complete account of Landau orbits [55], being equivalent to other methods for larger values of the magnetic field [15,56]. Although the effective coupling constants are not gauge invariant due to the explicit dependence on the gluon propagator, it might be that the full gauge invariant set of effective hadron couplings can only be

recovered by considering the complete set of physical mechanisms for QCD, not only quark polarization performed in the present work. It is interesting to note that the effect of the auxiliary fields on quark-quark effective interactions is of higher order, such as for example quark-vector and axial mesons interactions due to pion exchange. These corrections can be obtained by expanding the quark determinant considered above up to the second order in the a.f., which can be integrated out latter in a saddle point approximation. These terms are of higher order in S_0^n , i.e., $n \geq 2$, and consequently numerically smaller in the large quark mass limit.

ACKNOWLEDGMENTS

The author acknowledges short discussions with G. I. Krein, P. Bedaque, and C. D. Roberts.

-
- [1] C. Patrignani *et al.* (Particle Data Group), *Chin. Phys. C* **40**, 100001 (2016) and 2017 update.
- [2] J. J. Sakurai, *Ann. Phys. (N.Y.)* **11**, 1 (1960).
- [3] M. Bando, T. Kugo, and K. Yamawaki, *Phys. Rep.* **164**, 217 (1988).
- [4] U. G. Meissner, *Phys. Rep.* **161**, 213 (1988).
- [5] M. C. Birse, *Z. Phys. A* **355**, 231 (1996).
- [6] J. Eser, M. Grahl, and D. H. Rischke, *Phys. Rev. D* **92**, 096008 (2015); D. Parganlija, P. Kovacs, G. Wolf, F. Giacosa, and D. H. Rischke, *Phys. Rev. D* **87**, 014011 (2013); D. Parganlija, F. Giacosa, and D. H. Rischke, *Phys. Rev. D* **82**, 054024 (2010).
- [7] Th. Fuchs, M. R. Schindler, J. Gegelia, and S. Scherer, *Phys. Lett. B* **575**, 11 (2003).
- [8] D. Djukanovic, J. Gegelia, and S. Scherer, *Int. J. Mod. Phys. A* **25**, 3603 (2010).
- [9] M. Lavelle and D. McMullan, *Phys. Rep.* **279**, 1 (1997); E. de Rafael, *Phys. Lett. B* **703**, 60 (2011).
- [10] A. W. Thomas, *Nucl. Phys. B, Proc. Suppl.* **119**, 50 (2003); R. D. Young, D. B. Leinweber, and A. W. Thomas, *Prog. Part. Nucl. Phys.* **50**, 399 (2003), and references therein.
- [11] B. D. Serot and J. D. Walecka, *Int. J. Mod. Phys. E* **06**, 515 (1997).
- [12] F. Klingl, N. Kaiser, and W. Weise, *Nucl. Phys. A* **624**, 527 (1997).
- [13] F. L. Braghin, [arXiv:1708.03632](https://arxiv.org/abs/1708.03632).
- [14] J. O. Andersen, W. R. Naylor, and A. Tranberg, *Rev. Mod. Phys.* **88**, 025001 (2016).
- [15] V. A. Miransky and I. A. Shovkovy, *Phys. Rep.* **576**, 1 (2015).
- [16] V. A. Miransky and I. A. Shovkovy, *Phys. Rev. D* **66**, 045006 (2002); G. S. Bali, F. Bruckmann, G. Endrodi, Z. Fodor, S. D. Katz, and A. Schafer, *Phys. Rev. D* **86**, 071502 (2012).
- [17] K. Fukushima and Y. Hidaka, *Phys. Rev. Lett.* **110**, 031601 (2013); F. Bruckmann, G. Endrodi, and T. G. Kovacs, *J. High Energy Phys.* **04** (2013) 112.
- [18] B. Chatterjee, H. Mishra, and A. Mishra, *Phys. Rev. D* **91**, 034031 (2015).
- [19] M. N. Chernodub, *Phys. Rev. Lett.* **106**, 142003 (2011).
- [20] K. Fukushima, D. E. Kharzeev, and H. J. Warringa, *Phys. Rev. D* **78**, 074033 (2008).
- [21] D. E. Kharzeev, *Prog. Part. Nucl. Phys.* **75**, 133 (2014); D. E. Kharzeev, *Annu. Rev. Nucl. Part. Sci.* **65**, 193 (2015).
- [22] E. V. Gorbar, *Phys. Lett. B* **695**, 354 (2011).
- [23] K. Tuchin, *Adv. High Energy Phys.* **2013**, 490495 (2013).
- [24] E. J. Ferrer, V. de la Incera, and A. Sanchez, *Phys. Rev. Lett.* **107**, 041602 (2011); E. J. Ferrer, V. de la Incera, and X. J. Wen, *Phys. Rev. D* **91**, 054006 (2015); E. J. Ferrer, V. de la Incera, I. Portillo, and M. Quiroz, *Phys. Rev. D* **89**, 085034 (2014).
- [25] R. L. S. Farias, K. P. Gomes, G. Krein, and M. B. Pinto, *Phys. Rev. C* **90**, 025203 (2014).
- [26] A. Ayala, C. A. Dominguez, L. A. Hernández, M. Loewe, and R. Zamora, *Phys. Lett. B* **759**, 99 (2016).
- [27] C.-F. Li, L. Yang, X. J. Wen, and G. X. Peng, *Phys. Rev. D* **93**, 054005 (2016).
- [28] M. A. Andreichikov, V. D. Orlovsky, and Y. A. Simonov, *Phys. Rev. Lett.* **110**, 162002 (2013).
- [29] F. L. Braghin, *Phys. Rev. D* **94**, 074030 (2016).
- [30] F. L. Braghin, [arXiv:1705.05926](https://arxiv.org/abs/1705.05926).
- [31] M. Kawaguchi and S. Matsuzaki, *Phys. Rev. D* **93**, 125027 (2016).
- [32] C. Schuren, F. Doring, E. Ruiz Arriola, and K. Goetze, *Nucl. Phys. A* **565**, 687 (1993).
- [33] F. L. Braghin, *Eur. Phys. J. A* **52**, 134 (2016).
- [34] F. L. Braghin, *Phys. Lett. B* **761**, 424 (2016).
- [35] C. D. Roberts, R. T. Cahill, and J. Praschifka, *Ann. Phys. (N.Y.)* **188**, 20 (1988).

- [36] D. Ebert, H. Reinhardt, and M. K. Volkov, *Prog. Part. Nucl. Phys.* **33**, 1 (1994).
- [37] D. Binosi, L. Chang, J. Papavassiliou, and C. D. Roberts, *Phys. Lett. B* **742**, 183 (2015) and references therein.
- [38] P. Maris and C. D. Roberts, *Int. J. Mod. Phys. E* **12**, 297 (2003); P. Tandy, *Prog. Part. Nucl. Phys.* **39**, 117 (1997).
- [39] K.-I. Kondo, *Phys. Rev. D* **57**, 7467 (1998).
- [40] J. M. Cornwall, *Phys. Rev. D* **83**, 076001 (2011).
- [41] K. Higashijima, *Phys. Rev. D* **29**, 1228 (1984); V. A. Miransky, *Sov. J. Nucl. Phys.* **38**, 280 (1983); K.-I. Aoki, M. Bando, T. Kugo, M. G. Mitchard, and H. Nakatani, *Prog. Theor. Phys.* **84**, 683 (1990).
- [42] S. P. Klevansky, *Rev. Mod. Phys.* **64**, 649 (1992).
- [43] U. Vogl and W. Weise, *Prog. Part. Nucl. Phys.* **27**, 195 (1991).
- [44] L. F. Abbott, *Acta Phys. Pol. B* **13**, 33 (1982).
- [45] D. Becirevic, V. Lubicz, F. Mescia, and C. Tarantino, *J. High Energy Phys.* **05** (2003) 007; M. Jaminon and E. Ruiz Arriola, *Phys. Lett. B* **443**, 33 (1998).
- [46] W. Heisenberg and H. Euler, *Z. Phys.* **98**, 714 (1936), translated into English, arXiv:0605038.
- [47] G. S. Bali, F. Bruckmann, G. Endrődi, Z. Fodor, S. D. Katz, S. Krieg, A. Schäfer, and K. K. Szabó, *J. High Energy Phys.* **2** (2012) 44; G. Endrodi, *J. High Energy Phys.* **04** (2013) 023.
- [48] J. Schwinger, *Phys. Rev.* **82**, 664 (1951); **93**, 615 (1954).
- [49] H. B. O'Connell, B. C. Pearce, A. W. Thomas, and A. G. Williams, *Phys. Lett. B* **354**, 14 (1995).
- [50] For example, in C. Downum, T. Barnes, J. R. Stone, and E. S. Swanson, *Phys. Lett. B* **638**, 455 (2006).
- [51] J. C. R. Bloch, C. D. Roberts, and S. M. Schmidt, *Phys. Rev. C* **61**, 065207 (2000).
- [52] A. F. Krutov, R. G. Polezhaev, and V. E. Troitsky, *Phys. Rev. D* **93**, 036007 (2016) and references therein.
- [53] A. Ballon-Bayona, G. Krein, and C. Miller, *Phys. Rev. D* **96**, 014017 (2017).
- [54] G. S. Bali, F. Bruckmann, G. Endrődi, F. Gruber, and A. Schäfer, *J. High Energy Phys.* **04** (2013) 130.
- [55] T.-K. Chyi, C.-W. Hwang, W. F. Kao, G.-L. Lin, K.-W. Ng, and J.-J. Tseng, *Phys. Rev. D* **62**, 105014 (2000).
- [56] P. Watson and H. Reinhardt, *Phys. Rev. D* **89**, 045008 (2014).